

HYBRID CATALYSTS FOR ACETYLENES POLYMERIZATION PREPARED BY ANCHORING $[\text{Rh}(\text{cod})\text{Cl}]_2$ ON MCM-41, MCM-48 AND SBA-15 MESOPOROUS MOLECULAR SIEVES – THE EFFECT OF SUPPORT STRUCTURE ON CATALYTIC ACTIVITY IN POLYMERIZATION OF PHENYLACETYLENE AND 4-ETHYNYL-*N*-{4-[(TRIMETHYLSILYL)-ETHYNYL]BENZYLIDENE}ANILINE

Hynek BALCAR^{a1,*}, Jan SEDLÁČEK^{b1}, Jan SVOBODA^{b2}, Naděžda ŽILKOVÁ^{a2}, Jiří RATHOUSKÝ^{a3} and Jiří VOHLÍDAL^{b3}

^a J. Heyrovský Institute of Physical Chemistry, Academy of Sciences of the Czech Republic, Dolejškova 3, CZ-182 23 Prague 8, Czech Republic; e-mail: ¹ balcar@jh-inst.cas.cz, ² nadezda.zilkova@jh-inst.cas.cz, ³ jiri.rathousky@jh-inst.cas.cz

^b Department of Physical and Macromolecular Chemistry, Laboratory of Specialty Polymers, Faculty of Science, Charles University, Albertov 2030, CZ-128 40, Prague 2, Czech Republic; e-mail: ¹ jansedl@natur.cuni.cz, ² freedom@natur.cuni.cz, ³ vohlidal@natur.cuni.cz

Received June 18, 2003
Accepted August 8, 2003

Hybrid catalysts for polymerization of acetylenes were prepared by anchoring, *via* (3-amino-propyl)trimethoxysilane linker, the $[\text{Rh}(\text{cod})\text{Cl}]_2$ complex on siliceous mesoporous molecular sieves differing in the pore size and architecture (MCM-41, MCM-48 and SBA-15). In comparison with $[\text{Rh}(\text{cod})\text{Cl}]_2$ used as homogeneous catalyst, all hybrid catalysts exhibited comparable or even higher catalytic activity in the polymerization of phenylacetylene and 4-ethynyl-*N*-{4-[(trimethylsilyl)ethynyl]benzylidene}aniline. The initial polymerization rate increased with increasing accessibility of mesoporous surface of catalysts in the order: MCM-41 < MCM-48 < SBA-15. Molecular weights of the prepared polymers increased in reverse order suggesting suppression of the chain growth termination reactions by space limitations in the pores. No effect of catalyst support on the microstructure of formed polymers was found.

Keywords: Substituted acetylenes polymerization; Hybrid catalysts; Mesoporous molecular sieves; Polyacetylenes; Alkynes; Solid support; Supported catalysts; Rhodium.

Substituted polyacetylenes (polyvinylenes), polymers with conjugated polyene main chains attract attention because of their unique properties implicating applications in electronics and optics¹. The preparation of these polymers mainly consists in polymerization of corresponding substituted acetylenes with W-, Mo-, Rh- and Pd-based homogeneous catalysts^{2–4}. In the case of monomers of the phenylacetylene (PhA) type, Rh(I)(diene) com-

plexes (diene = cycloocta-1,5-diene (cod), norbornadiene) are most frequently used as polymerization catalysts since they exhibit high tolerance to polar functional groups, low sensitivity to moisture and oxygen and provide polymers with high microstructure uniformity (high content of *cis* double bonds and head-to-tail linkage)⁵. As catalyst residues in polymers may undesirably affect the polymer properties important for their applications, polymerization procedures minimizing the content of these residues in resulting polymers are of importance. Heterogeneously catalyzed polymerization induced by hybrid catalysts (known from the literature, *e.g.* in norbornene polymerization^{6,7}) is the most promising procedure meeting this demand. Recently, we have prepared this kind of catalysts by anchoring $[\text{Rh}(\text{cod})\text{X}]_2$ ($\text{X} = \text{Cl}, \text{OCH}_3$) on polybenzimidazole⁸ and mesoporous molecular sieves MCM-41 (refs^{9,10}). These catalysts afforded the heterogeneously catalyzed polymerization of PhA and its ring-substituted derivatives giving high-molecular-weight poly(phenylacetylene)s (PPhA). The study of PhA polymerization induced by both the hybrid catalysts showed that, in the course of reaction: (i) the polymer formed is continuously released into the liquid phase from which it can be easily isolated, (ii) the catalytic activity remains permanently bound to the solid phase (confirmed by separating the catalyst before completion of the polymerization and testing the liquid phase for activity), and (iii) no Rh leaching from hybrid catalysts occurs. Comparison of polymerization activity of hybrid catalysts based on the $[\text{Rh}(\text{cod})\text{Cl}]_2$ complex and differing in the support type showed a lower activity of the catalyst with polybenzimidazole support as compared with that prepared by anchoring the complex on mesoporous molecular sieves of the MCM-41 type. In comparison with $[\text{Rh}(\text{cod})\text{Cl}]_2$ used as homogeneous catalysts, the MCM-41-anchored $[\text{Rh}(\text{cod})\text{Cl}]_2$ provided comparable or even higher yields and considerably higher molecular weights of PPhA and reduced amounts of oligomeric by-products. Moreover, in comparison with any organic support, mesoporous molecular sieves possess other important advantages: (i) high mechanical and thermal stability, and (ii) well-defined pore size and architecture in mesoporous region.

In this paper we report on the preparation of hybrid catalysts by anchoring the $[\text{Rh}(\text{cod})\text{Cl}]_2$ complex on mesoporous molecular sieves MCM-41, MCM-48 and SBA-15 surface-modified by reaction with (3-aminopropyl)-trimethoxysilane (APTMS). The effect of the support pore size and architecture on the catalytic activity in polymerization of PhA and 4-ethynyl-*N*-{4-[(trimethylsilyl)ethynyl]benzylidene}aniline (ETMSEBA) tested as a monomer with a bulky substituent (Scheme 1) was particularly investigated.

EXPERIMENTAL

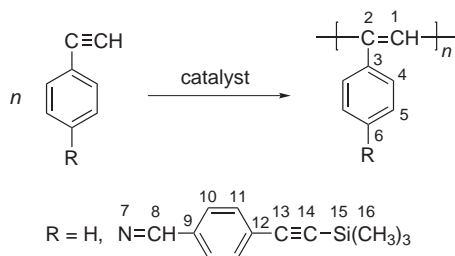
Materials

Molecular sieves of the MCM-41 type were synthesized by the homogeneous precipitation method using sodium silicate, hexadecyltrimethylammonium bromide and ethyl acetate. Details are given elsewhere^{11,12}. MCM-48 was synthesized by a modified literature procedure¹³ using Cab-O-Sil M5, sodium silicate, tetramethylammonium hydroxide and hexadecyltrimethylammonium bromide. SBA-15 was prepared from tetraethyl orthosilicate under acid conditions with Pluronic PE 10 400 (PEO₂₀PPO₄₇PEO₂₀) at 90 °C for 24 h (ref.¹⁴).

(3-Aminopropyl)trimethoxysilane (APTMS; Aldrich, 97%), phenylacetylene (PhA; Aldrich, 98%), di- μ -chlorobis[η^4 -cycloocta-1,5-diene]rhodium(I) ([Rh(cod)Cl]₂; Fluka, purum) were used as obtained. Tetrahydrofuran (THF; Riedel de Haen, purity 99.5+%) was freshly distilled from Cu₂Cl₂ and CaH₂. CH₂Cl₂ (Lachema, Czech Republic, p.a. grade) was distilled from P₂O₅ and stored over molecular sieves (Fluka, Type 4A). 4-Ethynyl-*N*-{4-[(trimethylsilyl)ethynyl]benzylidene}aniline was prepared by condensation of 4-[(trimethylsilyl)ethynyl]benzaldehyde with 4-ethynylaniline as described elsewhere¹⁵.

Hybrid Catalysts Preparation

Molecular sieves (MCM-41, MCM-48 or SBA-15, each 900 mg) were dried *in vacuo* at 300 °C for 6 h and, after cooling, suspended in CH₂Cl₂ (5 ml) under Ar atmosphere in a Schlenk vessel. Then APTMS (1.077 g, 6.0 mmol) was added in CH₂Cl₂ (15 ml) under vigorous stirring. After 3 h, the APTMS-modified molecular sieves (MCM-41/APTMS, MCM-48/APTMS or SBA-15/APTMS) were separated as a white solid by decantation, washed four times with 15 ml CH₂Cl₂ and dried in Ar stream at 40–50 °C. The APTMS-modified molecular sieves (817 mg) were suspended in CH₂Cl₂ (5 ml) and a yellow solution of [Rh(cod)Cl]₂ (20.1 mg, 0.041 mmol) in CH₂Cl₂ (11 ml) was added under vigorous stirring. The sieves turned yellow while the CH₂Cl₂ phase became colorless within 10 min. The stirring continued for 3 h and then the hybrid catalyst was separated by decantation, washed three times with CH₂Cl₂ (15 ml) and dried in Ar stream at 40–50 °C. In this way, the hybrid catalysts were prepared which will be denoted according to the type of support as follows MCM-41/APTMS/[Rh(cod)Cl]₂, MCM-48/APTMS/[Rh(cod)Cl]₂ and SBA-15/APTMS/[Rh(cod)Cl]₂.



SCHEME 1

Polymerization

A weighed amount of hybrid catalyst was suspended in a solvent (THF or CH_2Cl_2 , 1.5–2.5 ml) in a centrifuge vial equipped with a magnetic stirring bar. After 10 min, PhA or a solution of ETMSEBA in THF (1 ml) was added and the reaction mixture was allowed to react under stirring at room temperature. In all cases a high-molecular-weight polymer was formed which was continuously released into the liquid phase, which enabled monitoring of the reaction course by size exclusion chromatography (SEC). At a given time the reaction mixture was quickly centrifuged, supernatant (5 μl) was sampled, diluted with THF (0.5 ml) and the resulting solution (20 μl) was injected into SEC columns. The polymer content was determined from the area of the corresponding SEC peak using the final gravimetric polymer yield for calibration (*vide infra*). Simultaneously, molecular-weight characteristics of the polymer formed were obtained. After 7 h of polymerization, the supernatant (containing reaction products) was quantitatively separated from the hybrid catalyst and added to methanol (50 ml). The precipitated polymer, PPhA or poly[4-ethynyl-*N*-{4-[(trimethylsilyl)ethynyl]-benzylidene}aniline], (PETMSEBA), was washed several times with methanol/THF (4:1 by volume), dried *in vacuo* at room temperature and its yield was determined by gravimetry. The supernatant after polymer isolation was evaporated to dryness at room temperature. In this way, pure PhA-oligomers were obtained the yield of which was determined by gravimetry. The supernatant after PETMSEBA isolation gave the solid containing both ETMSEBA oligomers and unreacted ETMSEBA: the composition of the solid and the yield of oligomers were determined by SEC.

The used concentrations were (i) in PhA polymerizations: initial monomer concentration, $[\text{M}]_0 = 0.6 \text{ mol/l}$; concentration of hybrid catalyst, $c_{\text{cat}} = 15 \text{ g/l}$, *i.e.* $[\text{Rh}] = 1.5 \text{ mmol/l}$, (ii) in ETMSEBA polymerizations: $[\text{M}]_0 = 0.15 \text{ mol/l}$; $c_{\text{cat}} = 30 \text{ g/l}$, *i.e.* $[\text{Rh}] = 3 \text{ mmol/l}$.

Homogeneous polymerizations initiated with $[\text{Rh}(\text{cod})\text{Cl}]_2$ were performed similarly using the same values of $[\text{M}]_0$ and $[\text{Rh}]$.

Techniques

^1H NMR spectra of polymers were recorded on a Varian Unity INOVA 400. ^{29}Si CP MAS NMR spectrum of hybrid catalyst was measured on a Bruker MAS Spectrometer 500 MHz Widebore (ramp cross polarization, 4 mm probe, 9000 scans). Adsorption isotherms of nitrogen at 77.35 K were measured with a Micromeritics ASAP 2010 instrument. Prior to adsorption measurements, all the samples were degassed at 200 °C until a pressure of 0.1 Pa was attained. Scanning electron microscopy (SEM) (apparatus Jeol JSM 5500LW) was used for determination of size of molecular sieves particles. Low-angle X-ray powder diffraction ($2\theta = 1\text{--}10^\circ$) recorded on Siemens D5005 with $\text{CuK}\alpha$ was used to check the long-range ordering of the mesoporous molecular sieves studied.

SEC analyses were carried out on a TSP (Thermo Separation Products, Florida, U.S.A.) chromatograph fitted with a UV detector operating at 254 nm. A series of two PL-gel columns (Mixed-B and Mixed-C, Polymer Laboratories, Bristol, U.K.) and THF (flow rate 0.7 ml/min) were used. Weight-average molecular weights (M_w) and number-average molecular weights (M_n) relative to polystyrene standards are reported.

RESULTS AND DISCUSSION

Hybrid Catalyst Preparation and Characterization

XRD data (Fig. 1) of all mesoporous materials synthesized confirmed well-developed mesoporous structures of hexagonal (MCM-41, SBA-15) or cubic (MCM-48) symmetry. The particle size ranged from 1 to 3 μm for all the materials used (SEM). ^{29}Si CP MAS NMR spectra of APTMS-modified molecular sieves confirmed that in all cases APTMS was bound to the surface by reaction of $(\text{MeO})_3\text{Si}$ groups with surface OH groups. Figure 2 shows the ^{29}Si CP MAS NMR spectrum of MCM-48/APTMS. In addition to the Q_4 and Q_3 bands at -109.5 and -101 ppm, respectively, bands at -60 and -67 ppm appeared in the spectrum which can be ascribed to $(\text{SiO})_2\text{Si}(\text{OMe})[(\text{CH}_2)_3\text{NH}_2]$ and

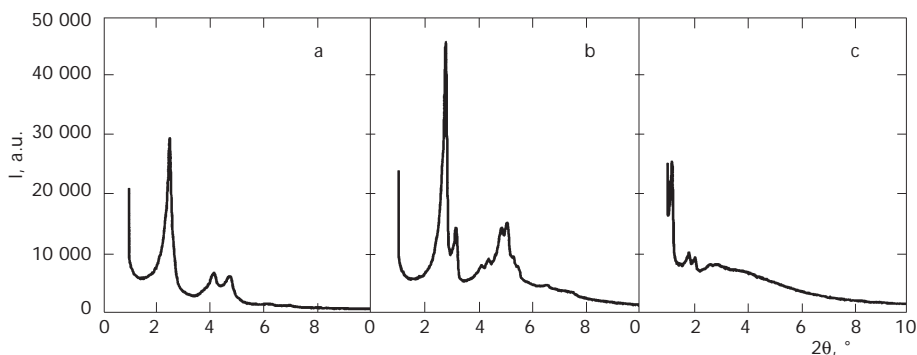


FIG. 1
X-Ray diffraction data of MCM-41 (a), MCM-48 (b) and SBA-15 (c)

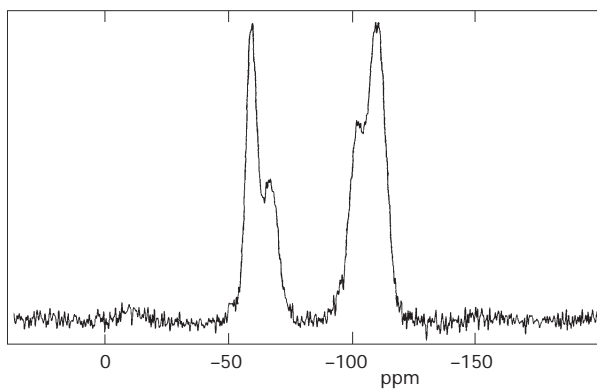


FIG. 2
 ^{29}Si CP MAS NMR spectrum of MCM-48/APTMS

($\text{SiO}_3\text{Si}[(\text{CH}_2)_3\text{NH}_2]$, respectively)¹⁶. Concentrations of APTMS in the APTMS-modified molecular sieves (by elemental analysis) are given in Table I.

Nitrogen adsorption isotherms at -196°C of both parent and APTMS-modified molecular sieves as well as corresponding texture parameters are presented in Fig. 3 and Table I. The BET surface area, S_{BET} , was evaluated from adsorption data in the relative pressure range from 0.05 to 0.15–0.20 (MCM-41 and MCM-48) and from 0.05 to 0.25–0.30 (SBA-15). The external surface area, S_{ext} , of all the materials was determined by the method of comparison plots¹⁷ using either macroporous silica gel Davisil 663XWP

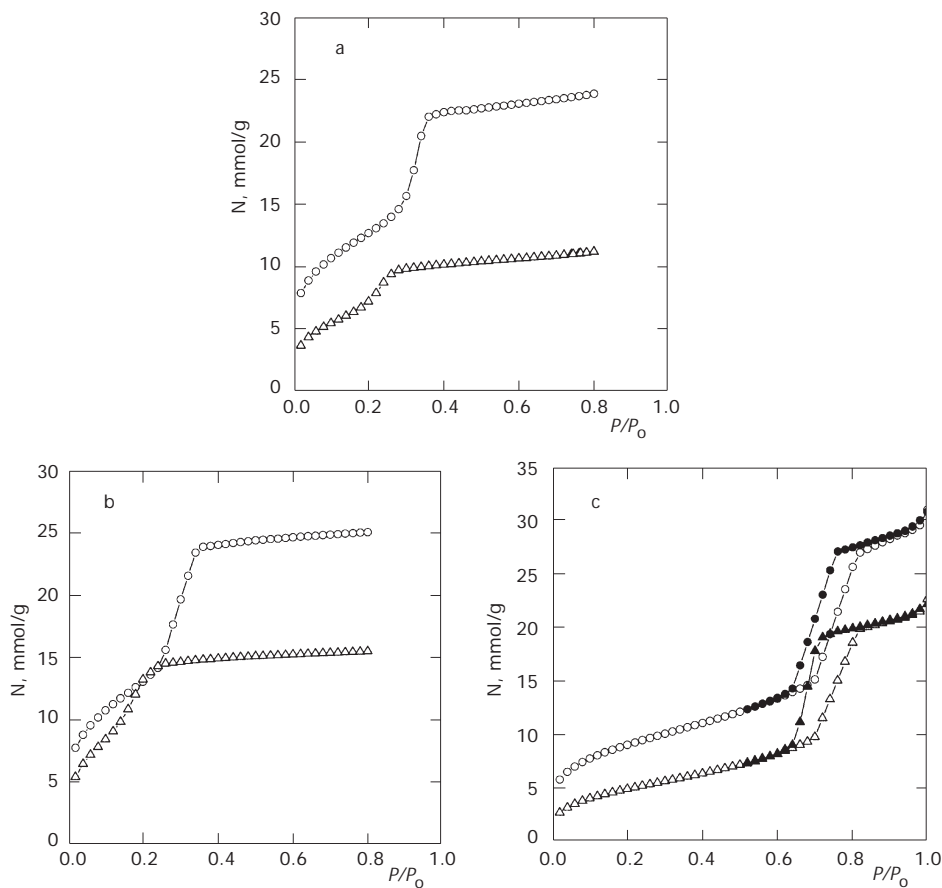


FIG. 3

Nitrogen adsorption isotherms of MCM-41 and MCM-41/APTMS (a), MCM-48 and MCM-48/APTMS (b), and SBA-15 and SBA-15/APTMS (c). Circles and triangles correspond to parent and modified materials, respectively (N , amount adsorbed; P/P_0 , relative pressure; open symbols, adsorption; full symbols, desorption)

(Supelco, $S_{\text{BET}} = 82.5 \text{ m}^2/\text{g}$) or its APTMS-modified form ($S_{\text{BET}} = 75.7 \text{ m}^2/\text{g}$) as reference adsorbents for parent and modified materials, respectively. Pertinent comparison plots are characterized by two linear parts, the first one corresponding to the formation of monolayer and the beginning of multilayer adsorption. The subsequent steep increase is due to the capillary condensation of nitrogen within mesopores. The second linear part corresponds to the plateau of the isotherm. As on this plateau the adsorption and desorption branches are identical multilayer adsorption is supposed to occur here. Therefore this part of comparison plots can be approximated by the straight line, $a = S_{\text{ext}} a_{\text{ref}} + V_{\text{me}}/v$, where a and a_{ref} are the amounts adsorbed on the sample under study and the relevant reference adsorbent, respectively, S_{ext} is the surface area which remains free after filling up the mesopores, *i.e.* the area of the external surface, V_{me} is the mesopore volume and v the molar volume of liquid nitrogen at $-196 \text{ }^\circ\text{C}$. The mesopore (*i.e.* internal) surface area, S_{me} , was calculated by subtracting S_{ext} from S_{BET} . For MCM-41- and MCM-48-based samples, the mean pore diameter, D_{me} , was determined using the formula $D_{\text{me}} = 4 V_{\text{me}}/S_{\text{me}}$. For SBA-15-based samples, the mesopore size distribution was calculated from the desorption branch of the isotherm using the BJH method, which provided the mesopore diameter D_{me} corresponding to the maximum of the distribution.

The calculations based on: (i) chemical composition of APTMS-modified materials provided by elemental analysis, and (ii) the determined surface area (S_{BET} ; Table I) showed that, in all prepared materials, at least two

TABLE I

Characteristics of parent and APTMS-modified mesoporous molecular sieves used as hybrid catalysts supports (S_{BET} , BET surface area; S_{ext} , external surface area; S_{me} , mesopore surface area; V_{me} , mesopore volume; D_{me} , mean mesopore diameter)

Sieves	APTMS concentration wt. %	S_{BET} $\text{m}^2 \text{ g}^{-1}$	S_{ext} $\text{m}^2 \text{ g}^{-1}$	S_{me} $\text{m}^2 \text{ g}^{-1}$	V_{me} $\text{cm}^3 \text{ g}^{-1}$	D_{me} nm
MCM-41	0	1032	104	927	0.718	3.1
MCM-48	0	1075	39	1035	0.821	3.2
SBA-15	0	720	79	641	0.878	7.7
MCM-41/APTMS	27.4	799	95	704	0.438	2.5
MCM-48/APTMS	27.8	909	23	886	0.510	2.3
SBA-15/APTMS	33.0	403	82	321	0.599	7.0

APTMS molecules are anchored on 1 nm^2 . From the ^{29}Si NMR data, the anchoring of one APTMS molecule by reaction with 2.2–2.3 surface OH groups (on average) can be roughly estimated^{10,18}. In the literature¹⁹, the average value of OH-group density on the surface of various silica materials is 4.9 OH groups per 1 nm^2 . We assume, therefore, that mesopore surface of all APTMS-modified sieves reported here is probably almost completely covered with the modifying agent.

$[\text{Rh}(\text{cod})\text{Cl}]_2$ reacts with APTMS-modified molecular sieves quantitatively. In all cases, complete disappearance of $[\text{Rh}(\text{cod})\text{Cl}]_2$ UV-VIS bands (350 nm, 390 nm, sh, 262 nm) in the supernatant was observed. For MCM-41/APTMS/ $[\text{Rh}(\text{cod})\text{Cl}]_2$, the Rh content was determined by elemental analysis and the results confirmed the quantitative character of $[\text{Rh}(\text{cod})\text{Cl}]_2$ anchoring¹⁰. Therefore, the Rh loading of all hybrid catalysts prepared was calculated from the supplied amount of $[\text{Rh}(\text{cod})\text{Cl}]_2$. All hybrid catalysts prepared were of the same Rh loading of 1 wt.%.

Catalytic Activity in Polymerizations of Phenylacetylene

Figure 4 shows time dependences of the yield, $Y(P)$, and weight-average molecular weight, M_w , of PPhA obtained in PhA polymerization in THF catalyzed with hybrid catalysts MCM-41/APTMS/ $[\text{Rh}(\text{cod})\text{Cl}]_2$, MCM-48/APTMS/ $[\text{Rh}(\text{cod})\text{Cl}]_2$, SBA-15/APTMS/ $[\text{Rh}(\text{cod})\text{Cl}]_2$ and with $[\text{Rh}(\text{cod})\text{Cl}]_2$ used as homogeneous catalyst under the same reaction conditions. It is seen that the $Y(P)$ vs time dependence for homogeneously catalyzed polymerization exhibits an induction period (Fig. 4a, curve 4), which is probably due to a slow dissociation of the dinuclear complex $[\text{Rh}(\text{cod})\text{Cl}]_2$ into the mononuclear catalytic species and/or their precursors. In the case of hybrid catalysts, the mononuclear Rh species are formed during the anchoring process¹⁰, which facilitates the initiation stage of polymerization as apparent from the absence of induction period (Fig. 4a, curves 1–3). The results of PhA polymerizations performed with the above catalysts in CH_2Cl_2 are given in Fig. 5. A low PPhA yield achieved in homogeneously catalyzed polymerization indicates that non-polar and non-coordinating CH_2Cl_2 is, in comparison with THF, evidently less efficient in $[\text{Rh}(\text{cod})\text{Cl}]_2$ dissociation and stabilization of mononuclear catalytically active species. On the other hand, high PPhA yields achieved with all hybrid catalysts in both the solvents used show that $[\text{Rh}(\text{cod})\text{Cl}]_2$ anchoring on mesoporous sieves leads to sufficiently stabilized catalytic species, the polymerization activity of which is high in both polar (THF) and non-polar (CH_2Cl_2) solvents. The initial rate of heterogeneously catalyzed PhA polymerization increases in both

the solvents used in depending on the hybrid catalyst in the order: MCM-41/APTMS/[Rh(cod)Cl]₂ < MCM-48/APTMS/[Rh(cod)Cl]₂ < SBA-15/APTMS/[Rh(cod)Cl]₂. This increase probably reflects an increase in the rate of diffusion of PhA into catalyst pores resulting from: (i) higher pore diameter of SBA-15, and (ii) higher penetrability of three-dimensional cubic MCM-48 in comparison with one-dimensional hexagonal MCM-41 support of a low pore diameter (see Table I). The molecular weight of PPhA prepared with hybrid catalysts in THF is only slightly higher than that achieved with [Rh(cod)Cl]₂ homogeneous catalyst: the highest rise in M_w was observed for

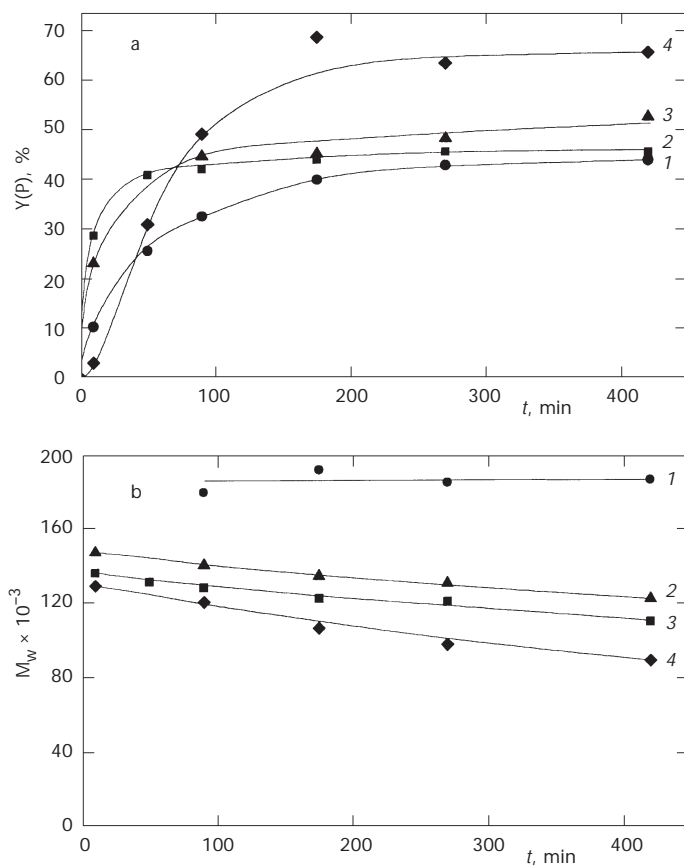


FIG. 4

Reaction time dependences of PPhA yield (a) and weight-average molecular weight, M_w (b) for PhA polymerization in THF. Catalysts: MCM-41/APTMS/[Rh(cod)Cl]₂ (1), MCM-48/APTMS/[Rh(cod)Cl]₂ (2), SBA-15/APTMS/[Rh(cod)Cl]₂ (3) and [Rh(cod)Cl]₂ (4). [Rh] = 1.5 mmol/l, [PhA]₀ = 0.6 mol/l, room temperature

PPhA prepared with MCM-41/APTMS/[Rh(cod)Cl]₂ (Fig. 4b). In CH₂Cl₂, the application of hybrid catalysts resulted in the production of PPhA of molecular weight about one order of magnitude higher than that achieved with [Rh(cod)Cl]₂ homogeneous catalyst. The polydispersity, M_w/M_n , in the range from 2.0 to 3.0 was found for PPhAs prepared with both hybrid and homogeneous catalysts in both solvents regardless of the polymerization time. A small decrease in PPhA molecular weight observed during polymerization in all experiments is probably due to the formation of shorter polymer chains in the later stages of polymerization when monomer concen-

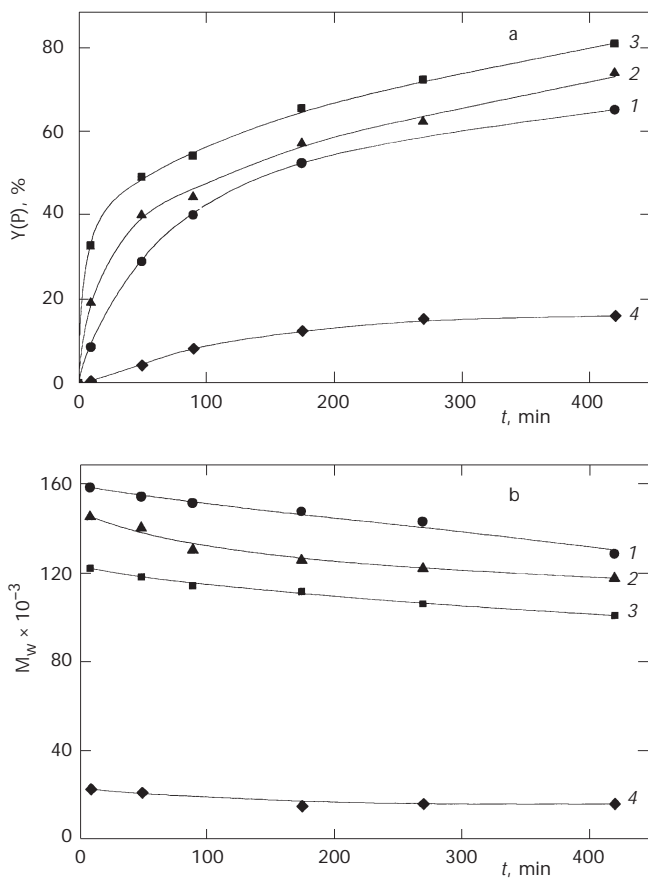


FIG. 5

Reaction time dependences of PPhA yield (a) and weight-average molecular weight, M_w (b) for PhA polymerization in CH₂Cl₂. Catalysts: MCM-41/APTMS/[Rh(cod)Cl]₂ (1), MCM-48/APTMS/[Rh(cod)Cl]₂ (2), SBA-15/APTMS/[Rh(cod)Cl]₂ (3) and [Rh(cod)Cl]₂ (4). [Rh] = 1.5 mmol/l, [PhA]₀ = 0.6 mol/l, room temperature

tration decreased and/or to slight polymer degradation, which is known to proceed in various solvents²⁰⁻²².

No differences in PPhA microstructure were found (IR and ¹H NMR) in dependence on: (i) catalyst, and (ii) polymerization solvent used. In all cases high-*cis*-PPhA with high microstructure uniformity was formed (for an example of ¹H NMR spectrum of PPhA prepared with SBA-15/APTMS/[Rh(cod)Cl]₂ in THF (Fig. 6)).

It is known that polymerization of PhA with Rh catalysts is always accompanied by undesirable formation of oligomers of molecular weights from 1000 to 2000. Figure 7 shows the final yield of oligomers obtained from experiments with [Rh(cod)Cl]₂ and with hybrid catalysts in both THF

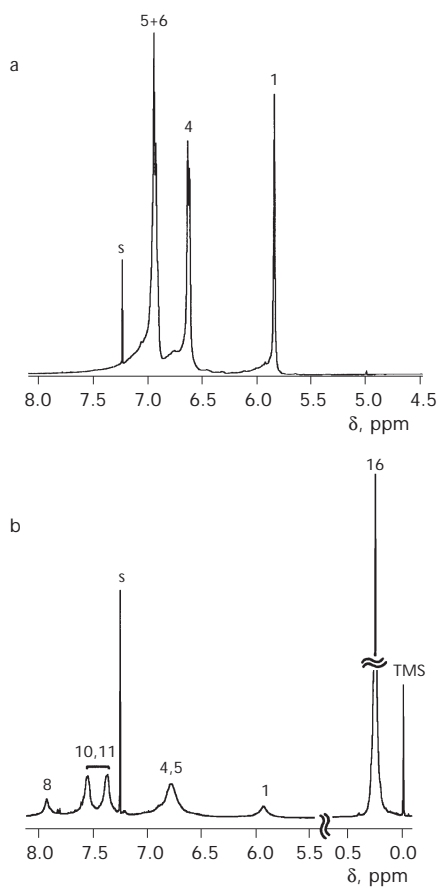


FIG. 6
¹H NMR spectra (in CDCl₃) of PPhA (a) and PETMSEBA (b) prepared with SBA15/APTMS/[Rh(cod)Cl]₂ in THF. For atom numbering, see Scheme 1; s = solvent

and CH_2Cl_2 . In both solvents, all the hybrid catalysts tested gave lower yields of PhA oligomers as compared with $[\text{Rh}(\text{cod})\text{Cl}]_2$. A similar positive effect of the $[\text{Rh}(\text{cod})\text{Cl}]_2$ anchoring on the suppression of oligomerization was observed in the previous study⁸, in which polybenzimidazole was used as hybrid catalyst support.

Catalytic Activity in Polymerizations of 4-Ethynyl-N-{4-[(trimethylsilyl)ethynyl]benzylidene}aniline

In order to find the impact of the monomer molecule size on the polymerization activity of mesoporous hybrid catalysts, we carried out the study of ETMSEBA polymerization catalyzed with hybrid catalysts and with $[\text{Rh}(\text{cod})\text{Cl}]_2$ in THF. ETMSEBA represents a monosubstituted acetylene with a relatively large rod-like substituent. Because of limited solubility of ETMSEBA, we adopted a lower monomer concentration than that used for PhA polymerization (see Experimental). The results of ETMSEBA polymerization are given in Fig. 8. It is seen that despite the bulky substituent, the polymerization with all hybrid catalysts proceeded smoothly under the formation of high molecular-weight PETMSEBA of expected polyvinylene structure (Scheme 1; confirmed by IR and ^1H NMR spectroscopy¹⁵), possessing a high microstructure uniformity and high-*cis* double-bond content independent of the catalyst used. Typical ^1H NMR spectrum of PETMSEBA prepared with hybrid catalyst is given in Fig. 6. Similarly to the PhA poly-

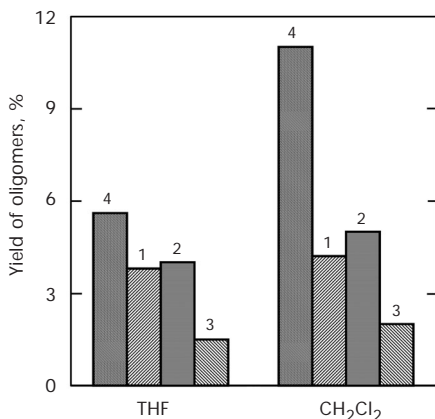


FIG. 7

Yields of oligomers resulting in PhA polymerization with MCM-41/APTMS/ $[\text{Rh}(\text{cod})\text{Cl}]_2$ (1), MCM-48/APTMS/ $[\text{Rh}(\text{cod})\text{Cl}]_2$ (2), SBA-15/APTMS/ $[\text{Rh}(\text{cod})\text{Cl}]_2$ (3) and $[\text{Rh}(\text{cod})\text{Cl}]_2$ (4) in THF and CH_2Cl_2 . $[\text{Rh}] = 1.5 \text{ mmol/l}$, $[\text{PhA}]_0 = 0.6 \text{ mol/l}$, room temperature, reaction time 7 h

merization, the polymerization of ETMSEBA was accompanied by the formation of oligomers (molecular weight = 2000–3000), the yield of which was up to 5% with all the catalysts tested, including the $[\text{Rh}(\text{cod})\text{Cl}]_2$ homogeneous catalyst. Contrary to the PhA polymerization in THF, in the ETMSEBA polymerization the hybrid catalysts provided: (i) a higher yield, and (ii) a substantially higher M_w of polymer prepared in comparison with the results obtained with $[\text{Rh}(\text{cod})\text{Cl}]_2$. The initial rate of ETMSEBA polymerization depending on the catalyst increased in the order $[\text{Rh}(\text{cod})\text{Cl}]_2 < \text{MCM-41/APTMS}/[\text{Rh}(\text{cod})\text{Cl}]_2 < \text{MCM-48/APTMS}/[\text{Rh}(\text{cod})\text{Cl}]_2 < \text{SBA-15}/$

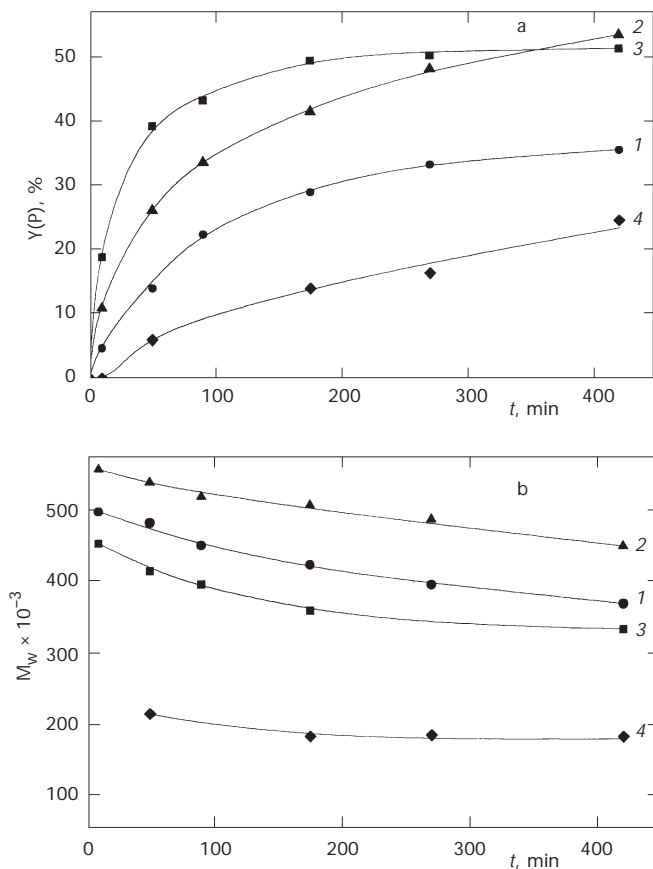


FIG. 8

Reaction time dependences of yield (a) and weight-average molecular weight, M_w , of polymer (b) for ETMSEBA polymerization in THF. Catalysts: MCM-41/APTMS/ $[\text{Rh}(\text{cod})\text{Cl}]_2$ (1), MCM-48/APTMS/ $[\text{Rh}(\text{cod})\text{Cl}]_2$ (2), SBA-15/APTMS/ $[\text{Rh}(\text{cod})\text{Cl}]_2$ (3) and $[\text{Rh}(\text{cod})\text{Cl}]_2$ (4). $[\text{Rh}] = 3.0 \text{ mmol/l}$, $[\text{ETMSEBA}]_0 = 0.15 \text{ mol/l}$, room temperature

APTMS/[Rh(cod)Cl]₂, *i.e.* similarly to PhA polymerization. The M_w values of PETMSEBA slightly increased, depending on hybrid catalysts, in the order SBA-15/APTMS/[Rh(cod)Cl]₂ < MCM-41/APTMS/[Rh(cod)Cl]₂ < MCM-48/APTMS/[Rh(cod)Cl]₂. Similarly to the PhA polymerization, the lowest values of M_w in the ETMSEBA polymerization were achieved with SBA-15/APTMS/[Rh(cod)Cl]₂ hybrid catalyst (Figs 4b, 5b, 8b), *i.e.* with the catalyst possessing the largest diameter of pores (Table I). It seems that the support structure exerts a certain effect on polymer molecular weight. This may indicate that limited space and specific environment of catalytic centres in mesoporous channels of hybrid catalysts contribute to suppression of termination of polymer chain growth and that this effect decreases with increasing diameter of pores in the hybrid catalyst support. However, in the absence of any knowledge about the mechanism of the spontaneous chain growth termination under homogeneous condition, the detailed interpretation of the observed data is not straightforward. As the chain growth termination is suppressed in narrow pores of hybrid catalysts (where steric hindrance and reduced monomer concentration can be expected), the termination by addition either of chain segments of polymer (oligomers) or of two monomer molecules to a propagating centre may be taken into account^{23,24}.

In our previous work¹⁰ we prepared MCM-41 with external surface passivated by reaction with Ph₂SiCl₂. By subsequent treatment with APTMS and [Rh(cod)Cl]₂, the hybrid catalyst was prepared in which the Rh species were located exclusively on the walls of mesoporous channels^{10,25}. This catalyst proved to be active in polymerization of PhA into high-molecular-weight PPhA and its polymerization activity was similar to that of MCM-41/APTMS/[Rh(cod)Cl]₂ with non-passivated external surface. Based on these findings, the conclusion was drawn that the PhA polymerization on MCM-41-supported catalyst proceeds within the support channels (at least prevalently). The results presented here, in particular: (i) the observed influence of the support pore size and architecture on the polymerization rate and molecular weight of polymers prepared, and (ii) the independence of polymerization activity on the external surface area of hybrid catalysts (Table I), can be regarded as additional evidence that the polymerization centres are located in the catalyst mesoporous channels.

CONCLUSIONS

Hybrid catalysts active in polymerization of phenylacetylene and of 4-ethynyl-*N*-{4-[(trimethylsilyl)ethynyl]benzylidene}aniline to high-molecular-

weight polymers of polyvinylene type were prepared by anchoring the $[\text{Rh}(\text{cod})\text{Cl}]_2$ complex on siliceous mesoporous molecular sieves MCM-41, MCM-48 and SBA-15 via (3-aminopropyl)trimethoxysilane. All hybrid catalysts prepared showed high polymerization activity: a comparable or even higher polymerization rate and higher polymer molecular weight compared with parent $[\text{Rh}(\text{cod})\text{Cl}]_2$. Both polymerization rate and molecular weight of polymers formed were found to depend on the support pore size and architecture: polymerization rate increased with increasing accessibility of mesoporous surface, molecular weight of polymers decreased with increasing pore size. On the other hand, the type of mesoporous molecular sieves had no effect on polymer microstructure: high-*cis* polyacetylenes with high microstructure uniformity were formed with all catalysts.

The authors thank Dr J. Čejka, Dr J. Dědeček and Dr L. Brabec (J. Heyrovský Institute) for XRD data, CP MAS NMR spectra of hybrid catalysts and SEM measurements, respectively, and to Dr J. Zedník (Charles University) for NMR spectra of polymers. Financial support from the Grant Agency of the Czech Republic (projects No. 203/02/0976 and No. 203/03/0824), the Grant Agency of the Charles University (projects No. 241/2002/B-CH/PrF and No. 228/2000/B-CH/PrF) and the Ministry of Education, Youth and Sports of the Czech Republic (project No. MSM 113100001) is gratefully acknowledged.

REFERENCES

1. Nalva H. S. (Ed.): *Handbook of Organic Conductive Molecules*. Wiley, New York 1996.
2. Ivin K. J., Mol J. C.: *Olefin Metathesis and Metathesis Polymerization*, p. 204. Academic Press, London 1997.
3. Musikhahumma K., Masuda T.: *J. Polym. Sci., Part A: Polym. Chem.* **1998**, *36*, 3131.
4. Balcar H., Sedláček J., Zedník J., Vohlídal J., Blechta V. in: *Ring Opening Metathesis Polymerization and Related Chemistry* (E. Khosravi and T. Szymanska-Buzar, Eds), NATO Science Series II, Vol. 56, p. 417. Kluwer Academic Publishers, Dordrecht 2002.
5. Tabata M., Sone T., Sadashiro Y.: *Macromol. Chem. Phys.* **1999**, *200*, 265.
6. De Clercq B., Lefebvre F., Verpoort F.: *New J. Chem.* **2002**, *26*, 1201.
7. Melis K., De Vos D., Jacobs P., Verpoort F.: *J. Mol. Catal. A: Chem.* **2001**, *169*, 47.
8. Sedláček J., Pacovská M., Rédrová D., Balcar H., Biffis A., Corain B., Vohlídal J.: *Chem. Eur. J.* **2002**, *8*, 366.
9. Balcar H., Sedláček J., Čejka J., Vohlídal J.: *Macromol. Rapid Commun.* **2002**, *23*, 32.
10. Balcar H., Čejka J., Sedláček J., Svoboda J., Zedník J., Bastl Z., Bosáček V., Vohlídal J.: *J. Mol. Catal. A: Chem.* **2003**, *203*, 287.
11. Kooyman P., Slabová M., Bosáček V., Čejka J., Rathouský J., Zukal A.: *Collect. Czech. Chem. Commun.* **2001**, *66*, 555.
12. Dědeček J., Žilková N., Čejka J.: *Collect. Czech. Chem. Commun.* **2001**, *66*, 567.
13. Hitz S., Prins R.: *J. Catal.* **1997**, *168*, 194.
14. Wang Y., Noguchi M., Takahashi Y., Ohtsuka Y.: *Catal. Today* **2001**, *68*, 3.
15. Balcar H., Sedláček J., Zedník J., Blechta V., Kubát P., Vohlídal J.: *Polymer* **2001**, *42*, 6709.

16. Bell T. A., Pines A. (Eds): *NMR Techniques in Catalysis*, p. 269. Marcel Dekker, New York 1994.
17. Čejka J., Žilková N., Rathouský J., Zukal A.: *Phys. Chem. Chem. Phys.* **2001**, 3, 5076.
18. Mercier L., Pinnavaia T. J.: *Adv. Mater.* **1997**, 9, 500.
19. Zhuravlev L. T.: *Langmuir* **1987**, 3, 316.
20. Karim S. M. A., Nomura R., Masuda T.: *Polym. Bull.* **1999**, 43, 305.
21. Sedláček J., Vohlídal J., Grubišic-Gallot Z.: *Makromol. Chem., Rapid Commun.* **1993**, 14, 51.
22. Vohlídal J., Rédrová D., Pacovská M., Sedláček J.: *Collect. Czech. Chem. Commun.* **1993**, 58, 2651.
23. Kishimoto Y., Eckerle P., Miyatake T., Kainosho M., Ono A., Ikariya T., Noyori R.: *J. Am. Chem. Soc.* **1999**, 121, 12035.
24. Havlíček J.: *M.S. Thesis*. Charles University, Prague 2003.
25. Rohlfing Y., Wöhrle D., Wark M., Schulz-Eckloff G., Rathouský J., Zukal A.: *Stud. Surf. Sci. Catal.* **2000**, 129, 295.